AD_____

AWARD NUMBER DAMD17-94-J-4320

TITLE: Structure/Function of Recombinant Human Estrogen Receptor

PRINCIPAL INVESTIGATOR: Larry E. Vickery, Ph.D.

CONTRACTING ORGANIZATION: University of California at Irvine
Irvine, California 92717-7550

REPORT DATE: November 1998

TYPE OF REPORT: Annual

PREPARED FOR: U.S. Army Medical Research and Materiel Command
Fort Detrick, Maryland 21702-5012

REPORT DOCUMENTATION PAGE

Form Approved
OMB No. 0704-0188

1. AGENCY USE ONLY *(Leave blank)*	2. REPORT DATE	3. REPORT TYPE AND DATES COVERED
	November 1998	Annual (1 Sep 97 - 31 Aug 98)

4. TITLE AND SUBTITLE
Structure/Function of Recombinant Human Estrogen Receptor

5. FUNDING NUMBERS
DAMD17-94-J-4320

6. AUTHOR(S)
Larry E. Vickery, Ph.D.

7. PERFORMING ORGANIZATION NAME(S) AND ADDRESS(ES)
University of California at Irvine
Irvine, California 92717-7550

8. PERFORMING ORGANIZATION REPORT NUMBER

9. SPONSORING / MONITORING AGENCY NAME(S) AND ADDRESS(ES)
U.S. Army Medical Research and Materiel Command
Fort Detrick, Maryland 21702-5012

10. SPONSORING / MONITORING AGENCY REPORT NUMBER

11. SUPPLEMENTARY NOTES

12a. DISTRIBUTION / AVAILABILITY STATEMENT
Approved for public release; distribution unlimited

12b. DISTRIBUTION CODE

13. ABSTRACT *(Maximum 200 words)*

14. SUBJECT TERMS
Anti-Estrogens, Tamoxifen, Receptor Structure, Steroid Binding, Receptor Purification, Breast Cancer

15. NUMBER OF PAGES
32

16. PRICE CODE

17. SECURITY CLASSIFICATION OF REPORT	18. SECURITY CLASSIFICATION OF THIS PAGE	19. SECURITY CLASSIFICATION OF ABSTRACT	20. LIMITATION OF ABSTRACT
Unclassified	Unclassified	Unclassified	Unlimited

FOREWORD

Opinions, interpretations, conclusions and recommendations are those of the author and are not necessarily endorsed by the U.S. Army.

____ Where copyrighted material is quoted, permission has been obtained to use such material.

____ Where material from documents designated for limited distribution is quoted, permission has been obtained to use the material.

____ Citations of commercial organizations and trade names in this report do not constitute an official Department of Army endorsement or approval of the products or services of these organizations.

____ In conducting research using animals, the investigator(s) adhered to the "Guide for the Care and Use of Laboratory Animals," prepared by the Committee on Care and use of Laboratory Animals of the Institute of Laboratory Resources, national Research Council (NIH Publication No. 86-23, Revised 1985).

____ For the protection of human subjects, the investigator(s) adhered to policies of applicable Federal Law 45 CFR 46.

✓ In conducting research utilizing recombinant DNA technology, the investigator(s) adhered to current guidelines promulgated by the National Institutes of Health.

✓ In the conduct of research utilizing recombinant DNA, the investigator(s) adhered to the NIH Guidelines for Research Involving Recombinant DNA Molecules.

____ In the conduct of research involving hazardous organisms, the investigator(s) adhered to the CDC-NIH Guide for Biosafety in Microbiological and Biomedical Laboratories.

_____

PI - Signature Date

Structure/Function Studies on Recombinant Human Estrogen Receptor

DAMD17-94-J-4320

Progress Report November 16, 1998

Larry E. Vickery, Principle Investigator
Mark E. Brandt, Co-investigator

Abstract

Interaction of the estrogen receptor with its ligands is mediated by a C-terminal region of the protein designated the hormone binding domain (HBD). We initiated structure-function studies in an attempt to improve our understanding of how estrogen activates the receptor and how antagonists inhibit its activity. We previously reported high yield expression of recombinant human estrogen receptor HBD, and our results suggest that the isolated HBD forms dimers in solution and undergoes conformational changes comparable to those in the full-length protein. Recent efforts have focused on 1) obtaining crystals of the HBD suitable for x-ray diffraction analysis, 2) computer assisted modeling of the structure of the HBD, and 3) fluorescence studies to monitor ligand-induced conformational changes. Small crystals of the HBD have been obtained, although these are not yet suitable for diffraction analysis. Lacking crystallographic data, we performed structural modeling of the HBD. The model predicts that the core of the HBD remains essentially unaffected by ligand binding. We have used fluorescence spectroscopy to test this hypothesis, and these results also suggest that the HBD core is largely unaffected by ligand binding: all three of the HBD tryptophan residues appear to be located in hydrophobic environments in the presence and absence of ligand. Trp383, located close to the estradiol binding site, was perturbed slightly by ligand binding. Studies using iodide as a quenching agent showed that estradiol binding increased the accessibility of Trp360, suggesting that ligand binding alters the conformational flexibility of the HBD. Taken together, the modeling and fluorescence studies, along with previous results from these studies, suggest that the major conformational changes induced by ligand binding may be confined to the N- and C-termini.

Table of Contents

INTRODUCTION

The estrogen receptors are nuclear proteins evolutionarily-related to the receptors for the other steroid hormones, for vitamins A and D, and for thyroid hormone (1,2). Binding of ligands to these receptors is the initial step in a complex series of events culminating in an interaction of the ligand-bound receptor with the transcription machinery and modulation of gene expression. These receptor proteins exhibit four distinct properties required to exert their actions: hormone binding, multimeric complex formation, sequence specific DNA binding, and transcriptional modulation. The currently proposed schematic structure of these receptor proteins (shown in Figure 1 for the product of the estrogen receptor-α gene), based on sequence similarities and deletion analyses (summarized in reference 2), suggests that these proteins fold into at least three separate structural and functional domains: (i) an N-terminal domain having a highly variable length and amino acid sequence and believed to mediate much of the transcriptional enhancement activity of the protein, (ii) a highly conserved central domain of ~80 amino acids involved in DNA-binding, and (iii) a less well conserved C-terminal domain of ~250 amino acids that is involved in ligand binding.

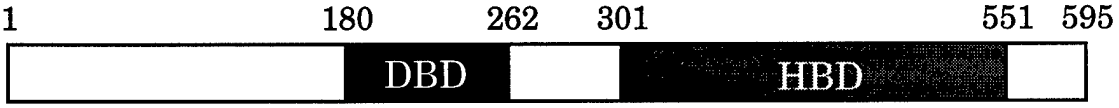

Figure 1. Schematic structure of the estrogen receptor-α. The locations of the N-terminal domain, DNA-binding Domain, and Hormone Binding Domain are shown using the amino acid numbering for the human protein.

The C-terminal hormone binding domain (HBD) is thought to contain many of the regulatory functions of the protein. Chimeric constructs containing fusions of fragments of the estrogen receptor with unrelated proteins such as the *myc* oncogene product, for example, display hormonal regulation of the activity of the fused gene products (3). This suggests that, even when removed from its normal environment, the HBD is not only capable of specific ligand binding, but may also retain the capacity to undergo the conformational changes that normally regulate the function of the receptor. Furthermore, the finding that the HBD can affect the activity of unrelated proteins suggests that the ligand-induced alteration in conformation may be a fundamental change in structure. Although some details remain obscure, comparison of the ligand-free human retinoid-X-receptor (RXR-α) and the ligand-bound human retinoic acid receptor (RAR-γ) and ligand-bound human estrogen receptor HBD structures (4-6) led to the suggestion that ligand binding to the nuclear-receptor family proteins alters the conformation of the C-terminus of the HBD, a region previously proposed to contain a conserved transcriptional activation function (7,8). In spite of the crystallographic data, however, the conformational changes that occur as a result of ligand binding remain poorly understood.

The nuclear receptor superfamily proteins form dimers. This property has at least two functional roles: most of the proteins in the family are thought to bind DNA as dimers, and dimer formation allows cooperative ligand binding, thereby narrowing the ligand concentration range required for full biological effect. The nature of the dimer interface of the full-length receptor protein is not established. The isolated DNA-binding domain has been shown to dimerize in the presence of DNA, suggesting that some of the dimerization interface resides within this portion of the protein; the isolated DNA-binding domain, however, is monomeric in solution. The HBD is also thought to play a role in dimerization. We have shown that the isolated estrogen receptor HBD forms dimers in solution (see 1996 and 1997 progress reports and ref. 9). However, the regions of the HBD that are involved in dimerization have not yet been fully mapped, and the role dimerization plays in the function of the protein has not yet been established.

Recently a second gene, designated estrogen receptor-β, was discovered in several mammalian species (10), including humans (11). The product of this gene is smaller than the estrogen receptor-α (477 versus 595 amino acids). The DNA binding domains of the two proteins exhibit a high degree of sequence similarity (~95%), while the hormone binding domain is fairly similar (~60% identity); the remainder of the proteins are quite divergent. Unless otherwise noted, however, all of the discussion included in this progress report refers to the estrogen receptor-α.

Current progress includes: 1) crystallization of an HBD construct, 2) comparison of an estrogen receptor HBD ligand-free homology model to the recently released estrogen receptor estradiol-bound crystallographic data, and 3) characterization of HBD fluorescence spectra in the presence and absence of different ligands.

List of abbreviations

The abbreviations used are: AEBSF, [4-(2-aminoethyl)-benzenesulfonylfluoride]; CD, circular dichroism; DEAE, diethylaminoethyl; DTT, dithiothreitol; DTNB, 5, 5′-dithio-bis-(2-nitrobenzoic acid); HBD, hormone binding domain; MBP, maltose-binding protein; RAR, retinoic acid receptor, RXR, retinoid-X-receptor; TED, Tris-EDTA-DTT, TNB, thio-2-nitrobenzoic acid.

MATERIALS AND METHODS

Supplies – Restriction endonucleases and other enzymes used for DNA manipulation were obtained from Boehringer-Mannheim Corp. (Indianapolis, IN), New England Biolabs, Inc. (Beverly, MA), Stratagene Cloning Systems (La Jolla, CA), or United States Biochemical Corp. (Cleveland, OH). Synthetic oligonucleotides were obtained from Operon Technologies (Alameda, CA) or Genosys Biotechnologies, Inc. (The Woodlands, TX). Bacterial growth media components were purchased from Difco (Detroit, MI); other reagents were obtained from Sigma Chemical Company (St. Louis, MO). Tritiated estradiol was obtained from Amersham and New England Nuclear. The estrogen antagonist *trans*-4-hydroxytamoxifen was a gift from Dr. Dominique Salin-Drouin (Laboratories Besins-Iscovesco) and ICI 182,780 was a gift from Dr. Alan Wakeling (ICI Pharmaceuticals).

Vector Construction – Unless otherwise noted, all DNA manipulations were carried out by standard techniques (13). As described in the previous progress reports, a DNA fragment coding for the human estrogen receptor hormone binding domain (amino acids 301-551) was generated by PCR from the HE0 estrogen receptor-α cDNA plasmid (14). The PCR fragment was digested with *Eco*RI and subcloned into the pMAL-c2 vector (New England Biolabs) which had been digested with *Xmn* I and *Eco*RI. Following isolation of the insert-containing plasmid, the entire HBD coding region was sequenced to confirm the absence of errors introduced by PCR amplification. The presence of the cDNA mutation Gly400Val (15) was verified by DNA sequencing; this mutation was reverted to wild-type using a PCR mutagenesis procedure (16), creating the plasmid pER08 (the Appendix contains a list of plasmids and their designations).

Protein products of pMAL-c2 derived plasmids consist of the maltose binding protein fused to the desired protein with a linker peptide consisting of $(Asn)_{10}$-Leu-Gly-Ile-Glu-Gly-Arg; the terminal four residues of the peptide comprise a Factor X_a cleavage signal. Factor X_a hydrolysis of the expressed fusion protein, however, resulted in heterogeneous, largely inactive peptides; we therefore modified the linker region to generate the sequence Asn-Gly, which can be cleaved by hydroxylamine (17). Bases encoding residues Leu-Gly-Ile-Glu of the Factor X_a recognition sequence were mutated to Asn codons by site-directed mutagenesis using the unique site-elimination procedure (18) with the Transformer kit from Clontech (Palo Alto, CA). The coding region of the mutagenesis product was sequenced; the modified DNA was found to encode a linker peptide of $(Asn)_{14}$-Gly-Arg. This plasmid was designated pER304. Unique site-elimination was then performed on pER304 to mutate Ser-305 to Glu, creating pER336. The product of hydroxylamine cleavage of the fusion protein from pER304, pER336, and a number of constructs derived from these plasmids retains Gly-Arg from the linker, the latter of which corresponds to the naturally occurring Arg-300.

Plasmids beginning at sites other than position 300 were constructed by subcloning PCR products into pMAL-c2, or into pMAL-INGR (pMAL-c2 in which the Glu from the Factor X_a site was mutated to Asn) in a manner similar to that described for pER08. Other plasmids discussed were constructed by site-directed

mutagenesis of previously existing plasmids containing appropriate characteristics.

Protein Expression and Purification – Competent TOPP2 cells (Stratagene) were transformed with the expression plasmids. Cells containing the appropriate plasmid were grown in TB media in the presence of 100 μg/ml ampicillin to an OD_{600} of ~1.7; protein expression was induced by the addition of IPTG to a final concentration of 0.25 mM and cultures were grown overnight at ambient temperature (usually ~27 °C).

The cells were harvested by centrifugation and frozen overnight at -20 °C. The cell pellets were resuspended in lysis buffer (50 mM Tris-HCl, 10 mM EDTA, 2 mM DTT, 1 mM AEBSF (Cal Biochem), pH 8.0, and 1 mg lysozyme/g of cells). After ~1 hr at ambient temperature, $MgCl_2$ was added to a final concentration of 120 mM and the lysate treated with DNase and RNase. The supernatant from a 40,000 x g centrifugation of the lysate was diluted 3-fold in TED buffer (20 mM Tris-HCl, 1 mM EDTA, and 1 mM DTT, pH 7.3) and applied to a DEAE-cellulose column (Whatman). The flowthrough from the DEAE-cellulose column was applied to an amylose resin column (New England Biolabs). After washing with 2-4 column volumes of TED containing 0.2 M NaCl, the fusion protein was eluted with 10 mM maltose in the same buffer.

The eluted protein was diluted 5-fold and applied to a DEAE-Sepharose column (Pharmacia). This column was washed with 5 column volumes of TED containing 0.05 M NaCl, and the protein was eluted with either a linear NaCl gradient (0.05-0.2 M NaCl; the fusion protein eluted at 0.13-0.16 M NaCl) or with 0.15 M NaCl in TED buffer. The fusion protein was then concentrated to ~20 mg/ml by precipitation with 60% ammonium sulfate or ultrafiltration (Amicon Centriprep) and was digested for 60-72 hours at ambient temperature with hydroxylamine (final concentration: 2 M hydroxylamine-HCl, 0.2 M Tris-HCl, pH 9.0). The cleaved HBD peptide was separated from the maltose binding protein by Sephadex G-100 gel filtration chromatography.

The final preparation of the purified pER304 or pER336-derived HBD peptide was stable and could be stored at 4 °C or -70 °C for several months. Some of the other constructs yielded unstable proteins (see subsequent sections).

Spectroscopy – All spectroscopy was performed at ambient temperature. Absorbance spectra were obtained using a Cary 1 spectrophotometer calibrated with $K_3Fe(CN)_6$ assuming ε_{420} = 1,020 $(M \cdot cm)^{-1}$. The concentration of purified MBP-HBD fusion protein and of isolated HBD peptide were determined spectrophotometrically assuming ε_{280} = 89,365 $(M \cdot cm)^{-1}$ for the fusion protein and 23,745 $(M \cdot cm)^{-1}$ for the HBD peptide; these values are based on a composition of 11 tryptophan and 20 tyrosine residues (fusion protein) or 3 tryptophan and 5 tyrosine residues (HBD peptide) predicted from the cDNA sequence and on average extinction coefficients for tryptophan (5615 $(M \cdot cm)^{-1}$) and tyrosine (1380 $(M \cdot cm)^{-1}$) (19,20). For the tryptophan mutants, the altered extinction coefficients were taken into account while determining concentrations.

Fluorescence spectra were recorded using an SLM-Aminco 8100

spectrofluorometer for samples in a 1 cm path length cell with bandpasses of 2 nm (excitation) and 4 nm (emission). Excitation spectra were collected using an emission wavelength of 335 nm with polarizers set to 0° (excitation) and 54.7° (emission). Emission spectra were obtained using an excitation wavelength of 283 or 295 nm with polarizers set to 54.7° (excitation) and 0° (emission). The relatively narrow excitation bandpass and the polarizing filters were used to prevent radiation-induced damage to the protein and other artifacts. In most cases five scans were collected, corrected against a rhodamine standard for lamp output and photomultiplier sensitivity, averaged, and baseline-corrected.

In order to more accurately determine the peak wavelength and the maximal intensity, spectra were fitted by least squares non-linear regression to a log-normal distribution (21):

$$I(\lambda) = I_0 e^{-\left\{\frac{\ln(2)}{\ln(\rho)^2}\left[\ln\left(1+(\lambda-\lambda_{max})\left(\frac{\rho^2-1}{\rho\Gamma}\right)\right)\right]^2\right\}} + C$$

where λ_{max} is the wavelength of maximal intensity, I_0 is the intensity at λ_{max}, Γ is the width of the spectrum at $I_0/2$, ρ is the peak asymmetry parameter, and C is the deviation of the baseline from zero.

Analytical Gel Filtration – The apparent molecular weight of the fusion protein and HBD were determined using a Pharmacia FPLC system and a Superdex 200 HR 10/30 gel filtration column (running buffer 20 mM Tris-HCl, 1 mM EDTA, 200 mM NaCl, pH 7.3). The column was calibrated using blue dextran to determine the void volume and with the following standard proteins: thyroglobulin (669 kDa), ferretin (440 kDa), catalase (232 kDa), aldolase (158 kDa), bovine serum albumin (69 kDa), ascorbate peroxidase (57.5 kDa), P450eryF (45.8 kDa), ovalbumin (43 kDa), MBP (40.4 kDa), rhodanese (33.3 kDa), chymotrypsinogen (25 kDa), ribonuclease A (13.7 kDa), and cytochrome c (12.4 kDa).

For the kinetic experiments, equimolar amounts of the fusion protein and HBD peptide were mixed and incubated at ambient temperature (~25°C). At various times aliquots were taken and subjected to FPLC gel filtration. For the experiments in the presence of ligand, the column was pre-equilibrated in the same running buffer with 50 nM of the relevant ligand, and 2 μM solutions of each protein pre-equilibrated overnight with 5 μM of the ligand. The integrated peak areas were corrected for extinction coefficient of the relevant protein species to determine the concentration of each species (*i.e.* fusion homodimer, HBD homodimer, or heterodimer) present at the time of injection (the relative amount of each species was assumed not to change during the chromatography). For experiments in the presence of ligand, the extinction coefficient of the protein was corrected for contributions of the bound ligand (assumed to be ~2,000 $(M \cdot cm)^{-1}$ for estradiol and ~15,000 $(M \cdot cm)^{-1}$ for 4-hydroxytamoxifen).

The rate constant for dissociation, k, was determined by least-squares non-linear regression of the first order rate equation:

$$D_t = (D_0 - D_f)e^{-kt} + D_f$$

where D_t is the concentration of one homodimer at time t, D_0 is the initial concentration of homodimer, and D_f is the final concentration of homodimer after the rearrangement had gone to completion. Half-life ($t_{1/2}$) for dissociation is defined as $\ln(2)/k$.

Free Cysteine Determination – The HBD peptide was diluted into phosphate buffer (0.1 M potassium phosphate, 1 mM EDTA, pH 7.25); added excess 5, 5′-dithio-bis(2-nitrobenzoic acid) (DTNB). In the presence of free sulfhydryl groups, DTNB covalently modifies the sulfhydryl and releases thio-nitrobenzoic acid (TNB). This results in a $\Delta\varepsilon_{412}$ of 14,000 $(M \cdot cm)^{-1}$.

Radioreceptor Assay – The HBD peptide was incubated overnight with various concentrations of [6,7-^{3}H]-estradiol at 4 °C in TED buffer including 0.2 M NaCl and 1 mg/ml porcine gelatin; bound and unbound steroids were separated using dextran-coated charcoal (0.625% charcoal, 0.125% dextran) in the same buffer without gelatin. In all experiments using purified and partially purified protein, the binding of radioactive estradiol in the presence of a 100-fold excess of unlabeled estradiol was equivalent to the non-specific binding observed in the absence of any added HBD protein. The data for bound and free steroid were directly fitted to the Hill equation (25):

$$[B] = \frac{B_{max}[F]^n}{(F_{0.5})^n + [F]^n}$$

using least squares non-linear regression analysis to estimate the $F_{0.5}$ (or K_d when n = 1), B_{max}, and n (Hill coefficient).

Molecular Modeling – The estrogen receptor-α HBD sequence was modeled using a World Wide Web-based homology modeling server (http://expasy.hcuge.ch/swissmod/SWISS-MODEL.html, see ref. 26-28). The RXR-α HBD structure (ExPDB database file 1lbd.pdb) was used as a template for the model. Examination of the original model indicated several suspect regions. These were corrected by altering the sequence alignment chosen by the computer algorithm. The modified model predicted an intrachain disulfide bond between residues 381 and 530. Removing this bond required altering the sequence to contain a Ser at position 381; this theoretical C381S mutant was used as the final model.

The model was assessed using the computer program SwissPDBViewer (version 3.1) running on PowerMacintosh computers; the measurements and graphics presented in the text were generated using this program.

RESULTS AND DISCUSSION

1. Crystallization Trials

One of the major goals of this project is to obtain structural information for the HBD using X-ray crystallographic analysis; this would be particularly useful for rational drug design. In order to determine the structure of the protein using this method, it is necessary to produce large amounts of homogeneous protein and to find conditions under which the protein will crystallize. The first of these goals has been met (see previous progress reports and Ref. 9). Several hundred milligrams of a number of different fusion proteins have been produced and apparently homogeneous cleavage of several of these in large quantities has been achieved. In contrast, finding conditions under which the HBD peptides will crystallize has proven to be rather difficult; recently, however, we were finally able to obtain crystals of one mutant form of the ER HBD.

In order for proteins to crystallize their tendency to remain in the solution must be lower than their concentration in the solution. However, if this disparity is too great, the protein will aggregate and precipitate in a non-ordered fashion. It is therefore necessary to find conditions where the protein will leave the solution in an orderly manner. In attempting to find these conditions, we have screened several thousand different buffer, precipitant, and ionic strength, and pH conditions using both fusion proteins and HBD peptides for several different mutants.

In late 1997, a paper describing the crystallization of the estrogen receptor HBD was published (22). They reported that they were unable to crystallize the native HBD; they were only able to obtain crystals after carboxymethylating the cysteine residues of the HBD. Their analysis of the structural information revealed that the cysteine at position 381 was modified the most extensively. In part based on this information, we attempted to crystallize an HBD peptide containing a C381S mutation (pER323).

We screened a number of conditions for the pER323 HBD peptide, and obtained small crystals from several of the conditions in the presence of the ligands estradiol and 4-hydroxytamoxifen. Because the 4-hydroxytamoxifen-HBD complex has not yet been solved, we began screening conditions in an attempt to find diffraction quality crystals for this complex.

A variety of conditions result in crystal formation for the pER323 HBD-4-hydroxytamoxifen complex; most involve the use of small alcohols (ethanol, isopropanol, ethylene glycol, and methyl-pentanediol). The largest crystals seem to form using ~20% t-butanol in 0.1 M sodium tricine buffer at pH 9.5. Thus far, however, the crystals, although quite long, are too narrow to be suitable for diffraction analysis. The larger crystals have dimensions of about 1000 x 30 x 10 μm.

The reason that the C381S HBD forms crystals, while the wild-type does not, is not clear. One possibility is that the Cys at position 381 may form interchain disulfide bonds. As presented in the 1997 progress report, the wild-type protein can

reversibly form disulfide bonds between dimers, based on both non-reducing SDS polyacrylamide gel electrophoretic and on gel filtration chromatographic data. However, pER323 (the C381S HBD construct) also forms disulfide multimers based on the same types of analyses (data not shown), but crystallizes far more readily than any other HBD construct tested. This suggests that the ability to form disulfide bonds between the dimeric HBD molecules in solution is not responsible for the resistance of the wild-type protein to crystallization. In addition, solution of the ER HBD structure by Tanenbaum *et al.* (6) revealed the presence of a disulfide bond formed between Cys530 residues of adjacent molecules. The Brzozowski and Tanenbaum structures are generally similar, and it is therefore unlikely that the disulfide bond causes a major structural change to the core of the protein, or that it plays much of a role in inducing crystallization.

An alternate possibility is that Cys381 may have a structural role in the protein. The mutation of the Cys to Ser was chosen to minimize the steric perturbation of the mutation. However, in addition to the altered behavior of pER323 under crystallization conditions, it also exhibits a much more rapid dimer exchange than any other construct tested ($t_{1/2}$ = 0.6 hours, which is 2.1-fold shorter than that of the expression product of the parent pER336 vector). It is therefore possible that the mutation of Cys381 to Ser (as well as the carboxymethylation chemical modification used by Brzozowski *et al.*, 22) may result in a small but significant conformational change. Although Tanenbaum *et al.* (6) report obtaining crystals of the unmodified protein, they obtained their actual x-ray data using a gold-adduct of the HBD (with both Cys381 and Cys417 having a gold atom bound) and used this form of the protein as their parent molecule in solving the structure.

Any conformational differences between the C381S mutant and wild-type protein, however, do not appear to result in diminished stability of the protein. The C381S mutant appears at least as stable as the wild-type HBD; it was expressed at high levels, and remains in solution at concentrations above 40 mg/ml.

Thus, we have obtained crystals for a mutant form of the estrogen receptor HBD. The mutation involves replacing the sulfur atom in Cys381 with an oxygen atom; this is a more conservative change than those introduced by the groups that have published ER HBD crystal structures. In addition, we have crystals for the HBD complexed with 4-hydroxytamoxifen; solving the structure for the HBD in the presence of this important class of antagonist compounds should yield important insights into the mechanism by which these compounds exert their effects.

2. Molecular modeling

Before the release of the crystallographic data for the ER HBD, we had performed some theoretical molecular modeling studies of the HBD. Comparison of our model with the experimentally-derived structure is useful, both 1) in order to assess the usefulness of current theoretical modeling techniques, and 2) in order to predict likely conformational differences between the ligand-bound structures and the thus far unsolved ligand-free form of the HBD. The crystal structures of the estrogen receptor HBD (6, 22) all have ligand bound; understanding how binding of

ligand changed the structure is a key element in understanding the role of the HBD in regulating the function of the estrogen receptor. In addition, increased understanding of the conformational changes induced by ligand binding will be helpful in designing more specific and more selective estrogen receptor modulators.

We used the structure of the related (~25% sequence identity) ligand-free RXR-α HBD (Protein Data Bank coordinate file 1lbd) to generate a three dimensional structural model for the estrogen receptor HBD. Manuel Peitsch has set up a computer server (http://expasy.hcuge.ch/swissmod/SWISS-MODEL.html, see ref. 26-28) which allows the entry of a protein sequence. The automated server aligns the sequence with sequences from previously solved homologous proteins, models the three dimensional structure of the entered sequence based on the known structures and then energy minimizes the resultant model. One potential problem with the automated system is that the sequence alignment chosen by the computer algorithm may not reflect the true alignment; however, the server allows the investigator to alter the alignment used. The alignment we used for the final models is shown in Figure 2. The alignment shown (*i.e.* the precise location of the gaps introduced) is slightly different from that based entirely on sequence identity.

```
                310       320  ±     330            340       350  Δ    360
hER-α     SKKNSLALSLTADQMVSALLDAEPP ILYSEYDPT     RPFSEASMMGLLTNLADRELVHMINW
                    11111111111                          33333333333333333333
                         111111111    2222222             333333333333333333
hRXR-α            -ane-mp-eri-e--lavepktetyveanmgln-s-pndpvtnicqa--kq-ftlve-
                     230       240       250       260       270       280 ¤

                370       380  ¤ ±  390  ¤Δ   400       410       420
hER-α     AKRVPGFVDLTLHDQVHLLECAWLEILMIGLVWRSMEHPGKLLFAPNLLLDRNQGKCVEG
          333         4444444444 555555555555      ||||   ||||666666
          33          4444444444 555555555555     ||||    ||||6666666
hRXR-α    ---i-h-se-p-d---i--rag-n-l-iasfsh--iavkdgi-l-tg-hvh--sahsa -
               290       300       310       320       330       340

                430       440   ±   4±0       460       470       480
hER-α     MVEIFDMLLATSSRFRM MNLQGEEFVCLKSIILLNSGVYTFLSSTLKSLEEKDHIHRVLDKITDTLI
          7777777777777777     8888888888888888         99999999999999999999
            7777777777777     88888888888888                  99999999999999
hRXR-α    vga---rv-telvskmrd-qmdkt-lg--ra-v-f-p        ds-g-snpaevealre-vyas-e
                350       360       370               380       390       400

          490       500  ±    510    ±  520   Δ   530       540       550
hER-α     HLMAKAGLTLQQQHQRLAQLLLILSHIRHMSNKGMEHLYSMKCKNVVPLYDLLLEMLDAHRLHA
          99999     000000000000000000000000000111111        222222222
          9999999      00000000000000000000     11111111111111111111
hRXR-α    ayckhkyp   e-pg-f-k---r-pal-sigl-cl---fff-ligdt-idtf-m---e-phqmt
                    410       420       430       440       450       460
```

Figure 2. Sequence alignment of the HBD for the human ER-α with human RXR-α. Dashes indicate identities with the ER-α sequence. The numbers between the sequences show the locations of the α-helices in the ER and RXR structures; the vertical lines indicate the positions of the β-sheet. The ¤ symbols indicate the three ER-α HBD tryptophan residues (note that Trp393 is not conserved in the RXR sequence). The Δ symbols indicate the ER residues that hydrogen bond to the estradiol molecule. The ± symbols indicate buried salt bridge residues present in the crystal structures.

Inspection of the model based this sequence alignment revealed the presence of an intramolecular disulfide bond between Cys381 and Cys530. Experimental data prior to the release of x-ray diffraction results had indicated that this was unlikely to exist in the unmodified protein. In addition, the crystal structures do not contain this disulfide bond, although the chemical modifications used in obtaining the crystals might have removed it. However, the model based on this sequence alignment that appeared more likely to be correct based on other criteria (described more completely below) than those based on other alignments. It proved necessary to use a theoretical C381S mutation to prevent the modeling software from inserting the disulfide bond.

The major assumption that underlies the homology modeling procedure is that related proteins have similar overall folds. In the case of the estrogen receptor and RXR structures, this turned out to be a good assumption. The resulting ER model has a core that appears similar to both the RXR structure and to the experimentally determined ER HBD structures (PDB coordinate file 1a52, see ref. 6, and file 1ere, see ref. 22; most of the discussion below will use the 1a52 structure). The model, superimposed on the 1a52 structure, is shown in Figure 3.

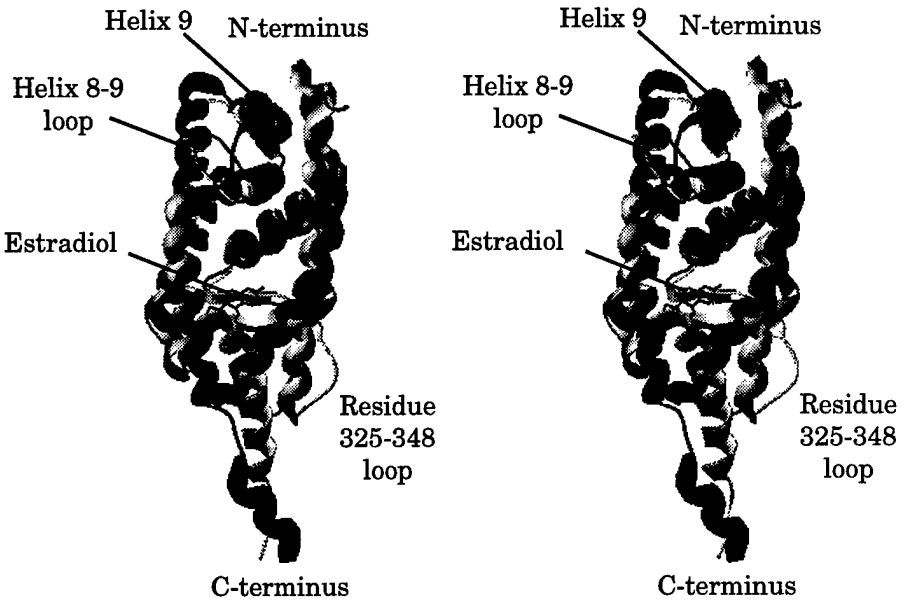

Figure 3. Stereoview of ER HBD model (light grey) superimposed on ER HBD crystal structure (dark grey). The loops between 325 and 348, and between 457 and 470 are indicated for the model. Note the penetration of the estradiol molecule into the backbone trace of the model.

The model does contain some significant deviations from the ER HBD structure. These deviations appear within loop regions (especially the loop between helices 8 and 9; ER residues 457 to 470), in the N-terminal region (prior to ER residue 350, especially the loop between 325 and 348), and in the C-terminal region (after residue 525). The loop linking helices 8 and 9 is poorly conserved between the ER and the RXR (note the gap in the sequence in Figure 2); in addition, this region had a high B-factor (indicating conformational flexibility) in the Tanenbaum *et al.* ER

HBD structure (6) and was completely disordered in the Brzozowski *et al.* ER HBD structure (22) suggesting that the differences in position between the structures and the model merely reflect the fact that this loop may assume different conformations in solution and in crystals. The deviations of the other regions, however, may be due to the fact that the ER HBD structure was solved with estradiol bound, while the RXR was crystallized in the absence of ligand; the altered positions of the chains in these regions may therefore be related to the conformational change that results from ligand binding (Figure 3, 4). We will discuss this possibility further below.

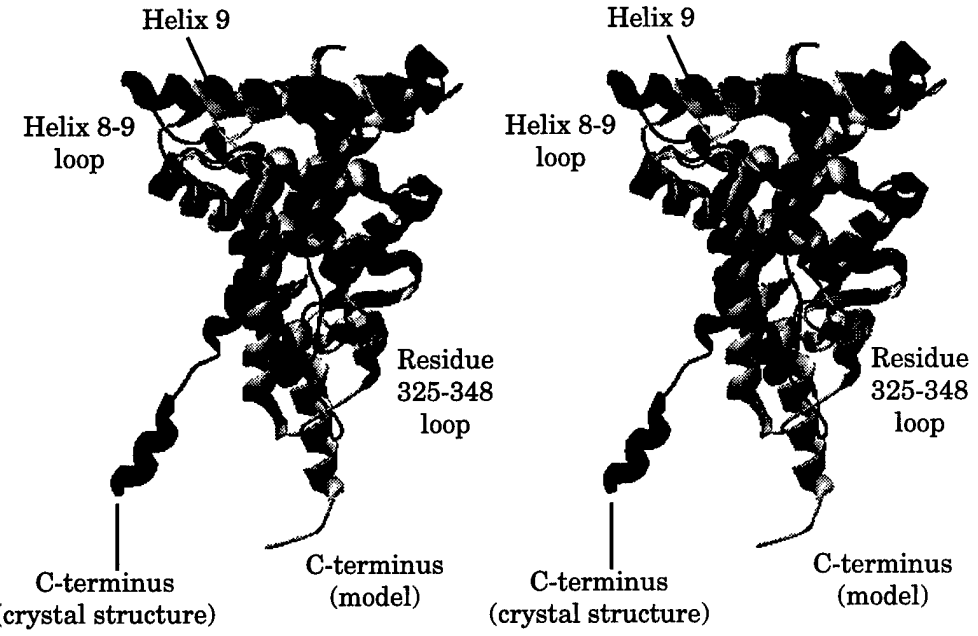

Figure 4. Stereoview of the ER HBD model (light grey) superimposed on ER HBD crystal structure (dark grey). The view in this figure is rotated 90° compared to Figure 3. The C-terminal helices in the crystal structure may be somewhat distorted by crystal packing contacts; however, at least some of the differences in this region are probably due to the presence of ligand in the crystal structure, and its absence in the model. The differences in the Helix 8-9 loop are probably due to a combination of multiple possible arrangements of this region and the fact that current modeling techniques have limited abilities to predict flexible regions.

One method of assessing the model is to compare the positions of the α carbons by measuring the root-mean-square (RMS) deviation of atoms. The RMS deviation for the Cα for residues all of the residues present in the model and visible in the experimentally determined structure (*i.e.* residues 309-544) is quite high: 7.76 Å. However, as noted above, the peptide contains several regions that exhibit significant deviations. The RMS excluding the widely deviating N- and C-termini (*i.e.* including only 350-525) is 3.76 Å; the RMS deviation for the sequence 350-525, and excluding the helix 8-9 loop is 2.02 Å. This suggests that the model is in fact a fairly close representation of the actual structure.

A second measure of the accuracy of the model is to examine the relative

positions of selected residue side chains. The alignment used was based in part on the location of conserved buried salt-bridge residues; other ER:RXR alignments with slightly greater numbers of identical residues resulted in buried charged residues without compensating charges of opposite signs, or in disruption of some of the buried salt bridges. Table 1 illustrates that much of the model is rather close to the actual structure, even for residues widely separated in the primary sequence. Note, for example, the similarity in inter-side chain distances for Trp393 and Phe445; neither of these residues is conserved in the RXR sequence.

Table 1
Inter-atom Distances for ER HBD Crystal Structure and ER HBD Model

Residues	ER-α HBD Estradiol-Bound Structure	ER-α HBD Ligand Free Model
Salt bridges		
Glu323 – Lys449 (εO – ζN)	4.0 Å	2.6 Å
Glu385 – Arg515 (εO – NH)	3.8 Å	3.5 Å
Glu444 – Arg503 (εO – NH)	2.4 Å	2.7 Å
Other selected residues		
Glu323 – Trp360 (εO – indole N)	3.9 Å	3.5 Å
Lys449 – Trp360 (ζN – indole N)	3.3 Å	5.2 Å
Trp393 – Phe 445 (closest side chain C)	3.8 Å	3.7 Å
Trp383 – Met522 (side chain C – S)	3.7 Å	4.9 Å
Trp383 – Met357 (side chain C – S)	5.5 Å	4.5 Å
Residues H-bonding to estradiol		
Glu353 – Arg394 (Cα – Cα)	13.8 Å	13.7 Å
Glu353 – His524 (Cα – Cα)	19.1 Å	18.5 Å
Arg394 – His524 (Cα – Cα)	22.1 Å	22.1 Å

The RXR HBD was crystallized in the absence of ligand, and the homology modeling software has no provision for the inclusion of anything other than amino acid residues. On the other hand, the ER HBD structures were solved in the presence of ligands. Because ligand binding is thought to result in conformational changes in the HBD, the positions of residues that directly contact the ligand might be expected to be differ considerably between the model and the actual structure. In the model, the side chains of Glu353, Arg394, and His524 (the three residues that form H-bonds to the estradiol hydroxyl groups) are in somewhat different positions from those in the actual structure. However, the α carbons of these residues are in very similar positions. Table 1 lists the Cα distances for these residues in the ER HBD model and in the crystal structure; these Cα distances are almost identical for

all three pairs of residues. This is a remarkable observation, and suggests that the conformational change induced by ligand binding does not actually involve the residues that seem to be most important for holding the ligand in place.

In the superimposition of the model and the crystal structure, the estradiol ligand of the structure intersects with the model backbone at positions 526-527 (Figure 5). The implication is that ligand binding forces a rearrangement of the backbone in this region. Moving this part of the backbone would also require moving the region near position 340, and suggests that the conformational changes induced by ligand binding do not affect the core of the HBD, but instead largely affect the N- and C-termini of the HBD.

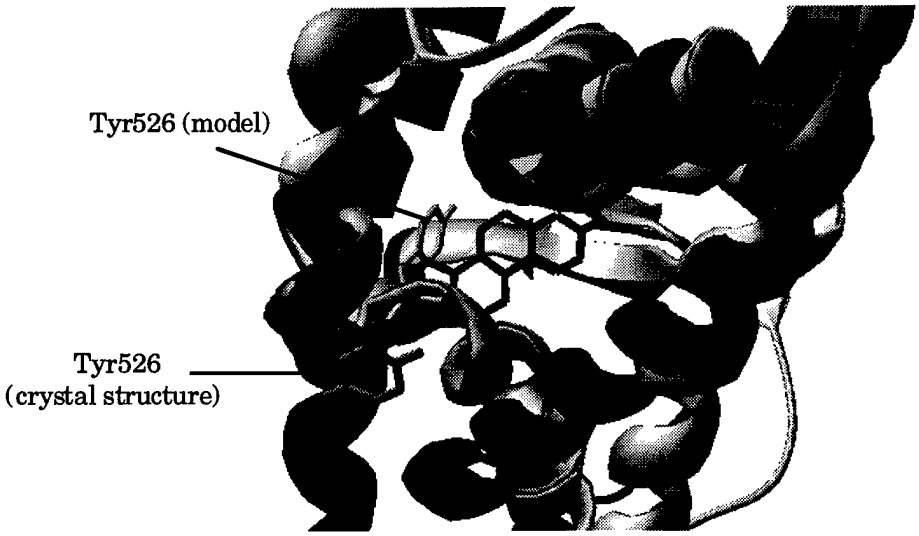

Figure 5. View of the ER HBD model (light grey) superimposed on ER HBD crystal structure (dark grey). The view in this figure is at higher magnification from a perspective similar to that in Figure 3. Note the penetration of the estradiol molecule of the crystal structure into the backbone of the model, and the differences in positioning of Tyr526. This rearrangement of the backbone may be one primary effect of ligand binding.

One related prediction of the model is a buried salt-bridge formed between Glu353 and Lys531. Clearly this does not exist in the ligand-bound structure, because Glu353 is one of the residues that contacts the ligand; these side chains are more than 20 Å apart in the crystal structure. It is possible that this predicted salt-bridge is important in stabilizing the ligand-free form of the receptor in the inactive conformation.

The modeling studies have several conclusions. 1) The ER HBD model is quite similar to the observed ER HBD crystal structure; many of the differences observed represent plausible predictions of the effect of ligand binding on the HBD conformation. 2) The α carbons of the residues that form hydrogen bonds to the estradiol hydroxyl groups (Glu353, Arg394, and His524) are in very similar relative positions in the model and in the structure, suggesting both that the conformation

around the ligand binding pocket for the RXR and ER is highly conserved and that the binding of ligand has little effect on the position of the peptide backbone near the residues that are most important in binding the ligand. 3) The model predicts that the conformational changes for the estrogen receptor HBD induced by ligand binding affect primarily the N- and C-termini, and not the core of the protein, and that the major source of these changes is a movement of the peptide backbone near position 526 to avoid a steric clash of the protein with the bound ligand. 4) The model predicts a buried charge interaction between Glu353 and Lys531 which is absent in the ligand-bound structure, and suggests that this interaction may stabilize the HBD in the inactive conformation.

3. Tryptophan Mutation Experiments

Fluorescence spectroscopy can be very revealing of the environment in the vicinity of the fluorophore. Unlike crystallographic data, which provides relatively static images, fluorescence is of considerable use for monitoring changes in protein conformation in solution. We attempted to use fluorescence to examine the environment of the intrinsic tryptophan residues in the ER HBD in the absence of ligand and in the presence of different ligands as a method for assessing the ligand-induced conformational changes.

Figure 6 shows the locations of the three tryptophan residues (positions 360, 383, and 393) in the ER HBD crystal structure (6). All three of the tryptophan residues are conserved among all of the human steroid receptors; Trp360 and Trp383 are conserved in RXR-α and in most (although not all) of the other nuclear receptors. The presence of three tryptophan residues complicates the analysis; we therefore decided to selectively remove the tryptophans in order to clarify the roles of the individual residues.

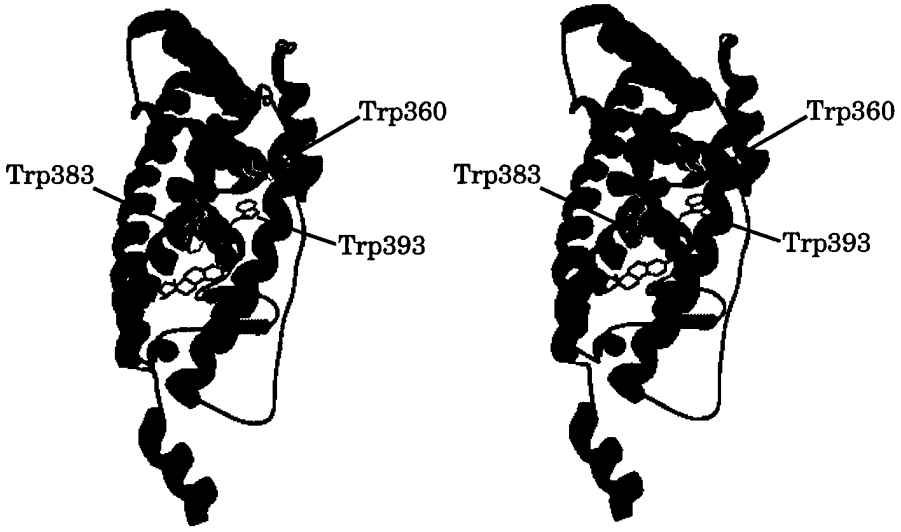

Figure 6. Stereoview of the ER HBD crystal structure (6); note that this structure includes a bound estradiol. The positions of the tryptophan residues are indicated.

Mutation of the tryptophan residues to phenylalanine was chosen since phenylalanine has negligible fluorescence and, while smaller than tryptophan, also has a hydrophobic and aromatic side chain. When the W360F mutant was expressed, however, it was found to be unstable. While it was possible to measure estradiol binding for the W360F fusion protein (K_d = ~1.5 nM, suggesting somewhat reduced affinity for estradiol), the protein denatured during the purification procedure. Mutation of Trp360 to tyrosine appeared to result in a more stable fusion protein, which exhibited an essentially wild-type affinity for estradiol. However, the W360Y mutant also denatured during purification. Addition of estradiol during the purification procedure in an attempt to stabilize the fusion protein had only a limited effect, and essentially all of the W360Y protein precipitated during the purification attempts. In one attempt a small amount of partially purified W360Y HBD peptide was obtained; however, analysis of the preparation suggested that it contained a mixture of folded and misfolded protein.

The reason for the instability of the Trp360 mutants is not entirely clear. While all of the steroid receptor proteins have tryptophan at this position, some other nuclear receptor superfamily members do not (for example, the corresponding residue in RAR-γ is a phenylalanine). It is possible that Trp360 assists in stabilizing the salt-bridge formed between Glu323 and Lys449, while neither tyrosine nor phenylalanine fully stabilize the local structure. The homology model generated by using the sequence of the W360F mutant appears essentially identical to the model based on the wild-type sequence; this may merely serve to illustrate a limitation of the homology modeling technique.

In contrast to the Trp360 mutants, the W383F, W393F, and W383F/W393F double mutant appeared to be quite stable. All three of these proteins expressed at high levels, and the purification procedure resulted in high yields of folded protein. The absorbance spectra of the mutants exhibited some differences from that of the wild-type HBD peptide, confirming the results of the plasmid DNA sequencing (Figure 7).

Radioreceptor assay analysis of the W383F, W393F, and W383F/W393F mutants indicated estradiol binding comparable to wild-type. All three of the proteins exhibited apparent K_d values of ~0.1-0.2 nM at low protein concentrations, and cooperativity with Hill coefficients of ~1.35-1.4 at higher protein concentrations.

The dimer dissociation kinetics of the mutants, however, differed somewhat from that of the wild-type protein, with $t_{1/2}$ for the dimer rearrangement of 3.9, 6.6, and 6.3 hours for the W383F, W393F, and W383F/W393F mutants, respectively (compared to 2.8 hours for the wild-type protein). None of these residues are located near the dimer interface. It is possible that mutation of the tryptophans (and of Trp393 in particular) may slightly alter the positioning of the N-terminus; previous studies in this laboratory have suggested that the N-terminus has a role in dimer interactions, in spite of the fact that the dimer interface is primarily located near the C-terminus (see 1997 progress report). Although the tryptophan mutations appear to affect the HBD dimer rearrangement, the presence of estradiol had a similar effect on the dimer dissociation kinetics to that observed for the wild-type protein: the $t_{1/2}$ increased by ~4-fold compared to that for the same protein without

ligand.

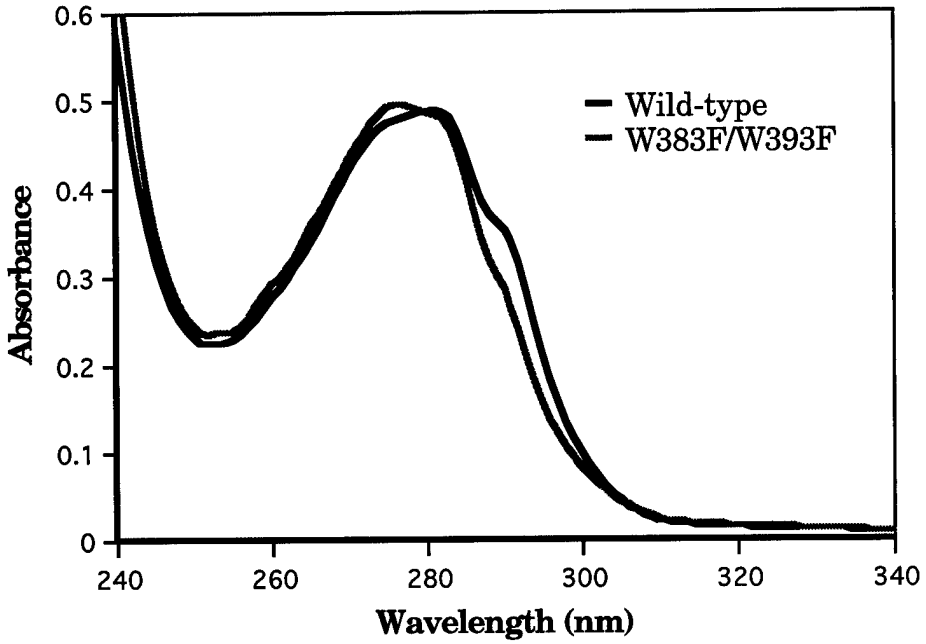

Figure 7. Absorbance spectra of the wild-type and W383F/W393F mutant. The spectra were normalized to the same A_{280}. Note the relative intensities at 276, 282, and 291 nm. The spectra of the tryptophan single mutants appeared intermediate between the two spectra shown here.

The fluorescence emission spectra for the wild-type and mutant proteins were collected using excitation at 295 nm (this wavelength was chosen to minimize tyrosine contribution to the spectrum); the spectra are shown in Figure 8. The smooth curves shown were generated by fitting the data to a log-normal distribution equation using non-linear regression (see Methods). This method allows more accurate determination of the peak position (λ_{max}) and provides information about the peak shape (21).

The emission data were further analyzed by comparison of the spectra to those obtained using N-acetyl-tryptophanamide (a model compound for tryptophan residues). The emission spectrum of N-acetyl-tryptophanamide varies with solvent composition; a plot of peak width at 50% of the intensity at λ_{max} *versus* λ_{max} for different solvents results in a linear relationship (21, 29). A calibration curve for N-acetyl-tryptophanamide and the data for the HBD peptides in aqueous buffer is shown in Figure 9. The data for the HBD peptides are all close to the line for N-acetyl-tryptophanamide, suggesting that the tryptophan residues are in homogeneous environments. The λ_{max} for N-acetyl-tryptophanamide is highest in an aqueous environment (352 nm), and decreases when exposed to various organic solvents. The λ_{max} values for the HBD peptides are given in Table 2, and are suggestive of an environment largely shielded from the aqueous medium.

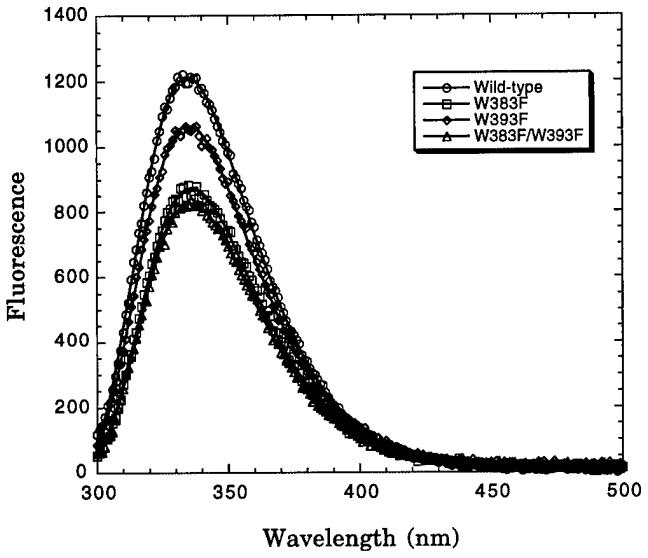

Figure 8. Fluorescence emission spectra for the ER wild-type and tryptophan mutant HBD peptides. All spectra were collected for 2 μM protein in the absence of ligand using excitation at 295 nm.

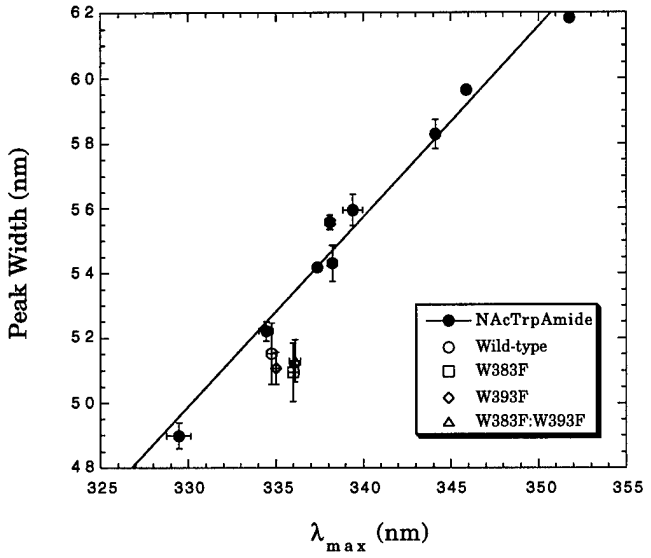

Figure 9. Plot of peak width (at 50% of maximum intensity) *versus* λ_{max} for N-acetyl-tryptophanamide and the HBD peptides in the absence of ligand. Each data point represents a minimum of four independent determinations; the error bars present the standard deviation of the measured values. The N-acetyl-tryptophanamide data represent spectra collected in aqueous buffer and different organic solvents; the most red-shifted data were obtained in aqueous buffer, while the most blue-shifted were obtained in dioxane. The data for the HBD peptides were collected in 10 mM Tris buffer (pH 7.4)

The spectrum for the W383F/W393F mutant corresponds to the spectrum from the Trp360 (assuming that tyrosine contributions are negligible for the protein when excited at 295 nm). The spectra for the remaining individual tryptophans, Trp383 and Trp393, cannot be measured directly due to instability of any HBD lacking the Trp360. However, subtracting the W383F spectrum from that of the wild-type protein, and subtracting the W383F/W393F spectrum from the W393F spectrum should yield spectra corresponding to the contribution of Trp393. Using these types of calculations, we obtained spectra for the three individual tryptophans (Figure 10).

Table 2
Emission Spectra Peak Positions

Protein	λ_{max} (nm)
wild-type	334.8 ± 0.3
W383F	336.0 ± 0.3
W393F	335.0 ± 0.2
W383F/W393F	336.1 ± 0.3
W383 alone (calculated)	330.9 ± 1.1
W393 alone (calculated)	335.6 ± 2.4

The data presented are mean ± SD for at least 10 independent measurements.

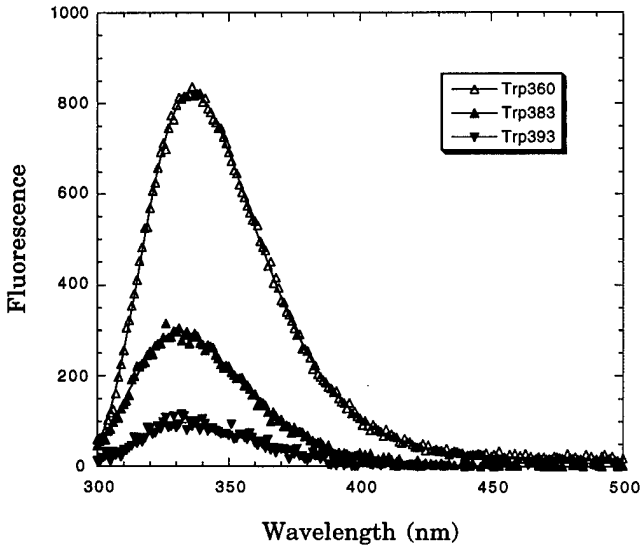

Figure 10. Comparison of the observed Trp360 spectrum (that of the W383F/W393F mutant) to calculated spectra for Trp383 and Trp393.

It is apparent from the spectra in Figure 10 that the quantum yield of the three tryptophans varies considerably: nearly 70% of the fluorescence intensity of the wild-type protein appears to be derived from Trp360, with Trp383 contributing about 25%, and Trp393 only about 8%. The crystal structure indicates that Trp360 is buried; the protection from solvent exposure may account for the relatively high quantum yield observed. However, the reason for the ~3-fold difference in quantum yield between Trp383 and Trp393 is less easily explained. In the crystal structure (for the ligand-bound ER HBD), and in the ER HBD model (based on the ligand-free RXR structure), both Trp383 and Trp393 appear partially solvent exposed with few obvious differences in local environment. The calculated λ_{max} for Trp383 appears slightly blue-shifted relative to the other tryptophan residues (by ~4 nm); however, this suggests a more hydrophobic environment, which is generally associated with an increase (rather than the observed decrease) in quantum yield.

Fluorescence is strongly dependent on changes in the local environment. We therefore tested the effects of ligand binding on the fluorescence spectra. Three ligands were used in most of the studies: the physiological ligand estradiol and two antagonists, ICI 182780 and *trans*-4-hydroxytamoxifen (Figure 11). The effects of estradiol and ICI 182780 on the fluorescence spectra were very small. A careful analysis of the data indicated a minor blue-shift of the spectra (≤~1 nm) for all of the peptides, and a small but reproducible increase in fluorescence intensity for two of the proteins. Figure 12 shows the effect of estradiol binding; similar results were obtained for ICI 182780. The increase in intensity was only observed for the wild-type and the W393F mutant, suggesting that binding of estradiol or ICI 182780 only perturbs the environment around Trp383. According to the crystal structure, Trp383 is near the entrance of the ligand binding pocket, and is fairly close to the bound estradiol; it is therefore reasonable that Trp383 would be affected by ligand binding. The lack of effect observed on the other two tryptophans is slightly surprising, however, and suggests that conformational changes induced by both agonist and antagonist ligands in the vicinity of those residues are very small.

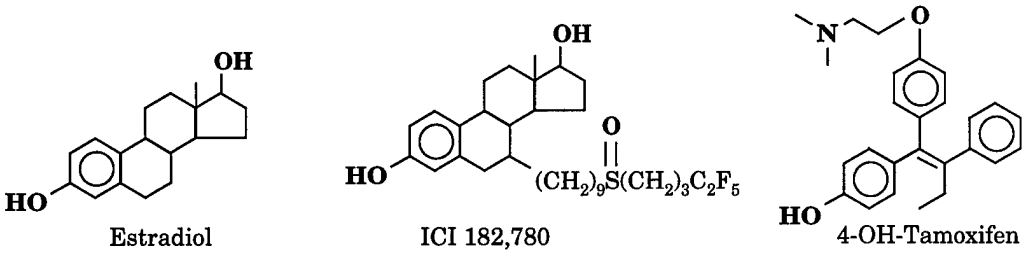

Figure 11. The structure of estradiol, and of the antagonist ligands ICI 182780 and 4-hydroxytamoxifen.

In contrast to the very small effect of estradiol and ICI 182780 on the fluorescence spectra, 4-hydroxytamoxifen resulted in a dramatic decrease in fluorescence intensity at the λ_{max} while slightly increasing the fluorescence at longer wavelengths for all three proteins (Figure 13, 14). The decrease in fluorescence observed was a specific effect; addition of an equimolar amount of estradiol partially reversed the effect.

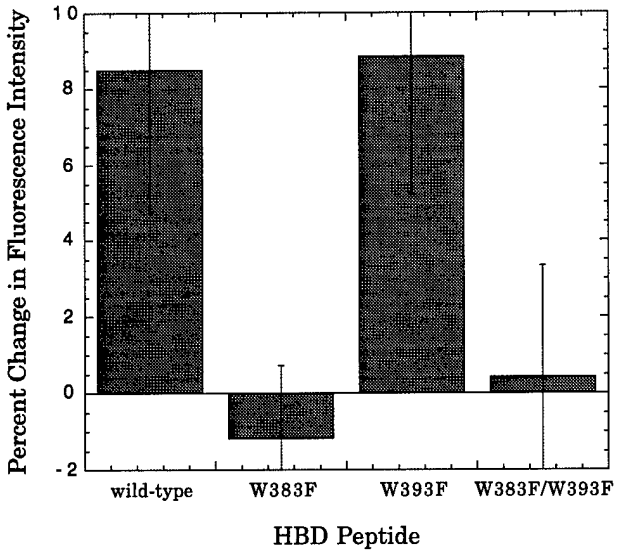

Figure 12. The effect of estradiol binding on peak fluorescence intensity. The data presented are the percent change in intensity in the same sample before and after addition of ligand. The data represent the mean ± standard deviation of at least 10 independent determinations.

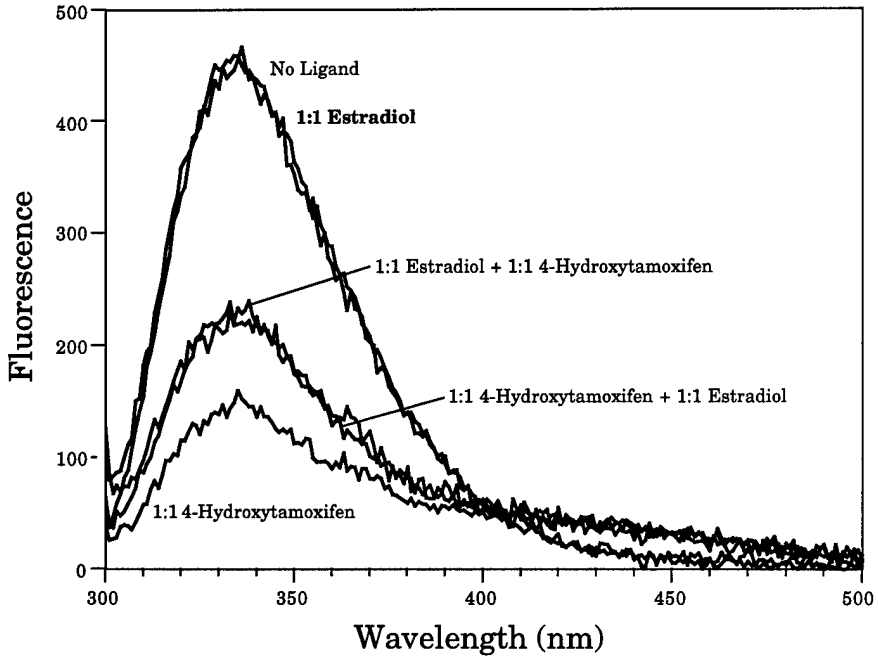

Figure 13. The effect of estradiol and 4-hydroxytamoxifen on the fluorescence of 1 μM wild-type HBD peptide. When added alone, 4-hydroxytamoxifen resulted in a marked decrease in the peak fluorescence; estradiol, when added either before or after the 4-hydroxytamoxifen partially reversed the effect. The spectra shown here are for the wild-type HBD; qualitatively similar results were obtained using the mutant HBD peptides.

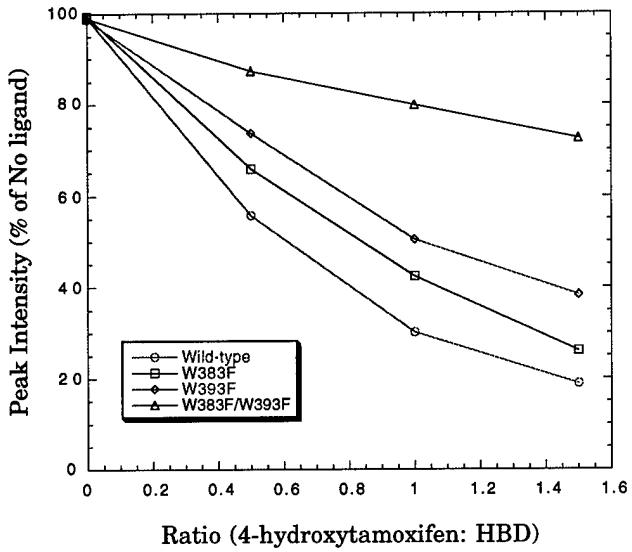

Figure 14. Dose-response curves for the effect of 4-hydroxytamoxifen on HBD fluorescence. In each case, the fluorescence intensity was normalized to the intensity observed for that peptide in the absence of ligand.

The fact that the antagonist ligand 4-hydroxytamoxifen decreases the tryptophan fluorescence in the HBD while the ligands estradiol and ICI 182780 do not suggests that the effect may be due to an energy transfer from the tryptophans to the aromatic 4-hydroxytamoxifen structure. The energy transfer event requires close proximity (*i.e.* actual binding of the ligand), but obtaining other useful information from the spectra is complicated by the differing quantum yields of the tryptophans.

A useful technique for examining the environment of the tryptophan residues involves the use of quenching agents. We tested iodide, an anionic quencher, and cesium, a cationic quencher. Cesium is known to be an inefficient quenching agent, and only negligible quenching was observed at concentrations as high as 1 M. Iodide, a much more efficient quenching agent than cesium, resulted in significant quenching, although it also required rather high concentrations. The results exhibited a surprisingly large degree of variability (note the large error bars in Figure 15), which makes interpretation somewhat difficult.

A Stern-Volmer plot of fractional decrease in fluorescence *versus* quencher concentration has a slope proportional to the accessibility of the fluorescent residue to the quenching agent. The Stern-Volmer constants measured for the various HBD peptides are given in Table 3.

For all of the peptides, quenching required much higher concentrations of iodide than was necessary for N-acetyl-tryptophanamide (note the much higher K_{SV} for N-acetyl-tryptophanamide in Table 3), suggesting that iodide access to the tryptophan

residues is significantly inhibited by the structure of the protein. Iodide is negatively charged; it is therefore possible that electrostatic repulsion could account for the reduced accessibility, although the tryptophans do not appear to be surrounded by acidic residues.

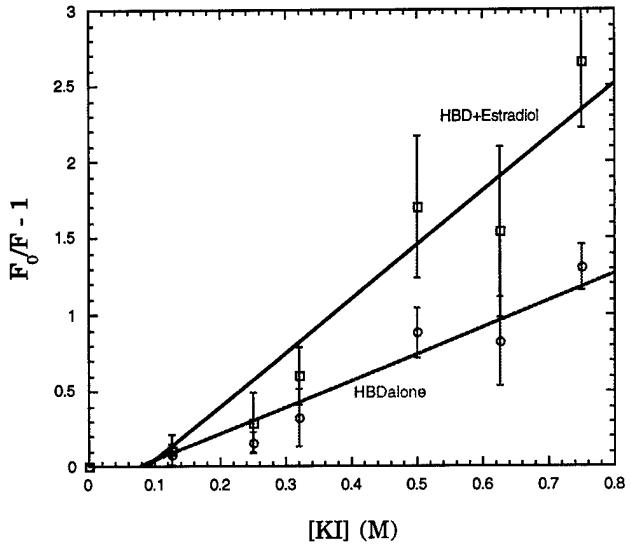

Figure 15. Stern-Volmer plot for iodide quenching of the wild-type HBD peptide in the presence and absence of estradiol. This is a plot of fractional fluorescence intensity (fluorescence in absence of quencher divided by fluorescence in the presence of quencher) *versus* potassium iodide concentration. The slope of the line is the Stern-Volmer constant; average values are given in Table 3.

Table 3
Stern-Volmer Constants for the HBD Peptides

Peptide	K_{sv}	K_{sv} with Estradiol
Wild-type	1.8	3.5
W383F	2.7	5.2
W393F	2.1	3.7
W383F/W393F	1.6	4.0
N-acetyl-tryptophanamide	13.0	13.0

Also for all of the peptides, addition of estradiol markedly increased the observed quenching. The mechanism for this increased accessibility of iodide to the

tryptophan residues is not clear. The binding of estradiol has a small effect on the fluorescence emission by Trp383, and does not appear to affect the fluorescence of the other two tryptophan residues, suggesting that structural changes in the vicinity of the tryptophans are very small. In contrast, the quenching results indicate that the accessibility of iodide increases dramatically in the presence of estradiol. Because the effect of estradiol on iodide quenching appears to be strongest for the W383F/W393F mutant, and because the single tryptophan remaining in this mutant accounts for ~70% of the fluorescent yield of the protein, it is likely that the estradiol effect on iodide quenching of the HBD is largely or exclusively due to changes in Trp360 fluorescence. Although ligand binding has no apparent direct effect on the environment of Trp360 (based on the similarity of spectral parameters for the W383F/W393F mutant in the absence and presence of ligand), ligand binding may allow iodide to gain increased access to Trp360, or to induce an additional conformational change near Trp360. Neither the crystal structure nor the homology model lend insight into what this change might be, and therefore additional studies of the protein in solution are probably necessary to understand the mechanism underlying the effect of estradiol binding on iodide quenching of tryptophan fluorescence.

The results of the tryptophan mutation studies lead to several conclusions. They suggest that the Trp360 has an important role in the structural core of the protein, while the HBD is much less sensitive to changes in the other tryptophans. Fluorescence spectroscopic studies on the wild-type HBD and tryptophan mutant HBD peptides suggest that all three of the tryptophans of the HBD are in largely non-aqueous environments. In the crystal structure, Trp383 and Trp393 appear partially solvent exposed; the fluorescence results suggest that for the HBD in solution, these residues may be somewhat more shielded from solvent than in the crystal. In addition, although the environments of Trp383 and Trp393 appear similar in the crystal structure, their quantum yields differ by ~3-fold.

Binding of estradiol appeared to directly affect the environment of Trp383 (which is in fairly close proximity to the ligand in the crystal structure), but did not appear to perturb the other two tryptophans. The fluorescence results thus appear to confirm the prediction of the theoretical model that the conformation of the core of the protein (which includes Trp360 and Trp393) is essentially unaffected by ligand binding. However, quenching studies revealed that iodide access to the HBD tryptophans (and to Trp360 in particular) increased with ligand binding, suggesting that ligand binding may actually increase the conformational flexibility of the protein core, while leaving the overall fold essentially unchanged.

REFERENCES

1. Evans, R.M. (1988) *Science* **240**, 889-895
2. Tsai, M.J. and O'Malley, B.W. (1994) *Annu. Rev. Biochem.* **63**, 451-486
3. Eilers, M., Picard, D., Yamamoto, K.R., and Bishop, J.M. (1989) *Nature* **340**, 66-68
4. Bourguet, W., Ruff, M., Chambon, P., Gronemeyer, H., and Moras, D. (1995) *Nature* **375**, 377-382
5. Renaud, J.P., Rochel, N., Ruff, M., Vivat, V., Chambon, P., Gronemeyer, H., and Moras, D. (1995) *Nature* **378**, 681-689
6. Tanenbaum, D.M., Wang, Y., Williams, S.P., and Sigler, P.B. (1998) *Proc. Natl. Acad. Sci. (USA)* **95**, 5998-6003
7. Danielian, P.S., White, R., Lees, J.A., and Parker, M.G. (1992) *EMBO J.* **11**, 1025-1033
8. Wurtz, J.M., Bourguet, W., Renaud, J.P., Vivat, V., Chambon, P., Moras, D., and Gronemeyer, H. (1996) *Nature Struct. Biol.* **3**, 87-94
9. Brandt, M.E. and Vickery, L.E. (1997) *J. Biol. Chem.* **272**: 4843-4849
10. Kuiper, G.G., Enmark, E., Pelto-Huikko, M., Nilsson, S., and Gustafsson J.A. (1996) *Proc. Natl. Acad. Sci.* **93**, 5925-5930
11. Mosselman, S., Polman, J. and Dijkema, R. (1996) *FEBS Lett.* **392**, 49-53
12. Seielstad, D.A., Carlson, K.E., Katzenellenbogen, J.A., Kushner, P.J., and Greene, G.L. (1995) *Mol. Endocrinol.* **9**, 647-658
13. Sambrook, J., Fritsch, E.F., and Maniatis, T. (1989) *Molecular Cloning: A Laboratory Manual* 2nd Ed. Cold Spring Harbor Laboratory Press, Cold Spring Harbor, New York
14. Kumar, V., Green, S., Staub, A., and Chambon, P. (1986) *EMBO J.* **5**, 2231-2236
15. Tora, L., Mullick, A., Metzger, D., Ponglikitmongkol, M., Park, I., and Chambon, P. (1989) *EMBO J.* **8**, 1981-1986
16. Nelson, R.M. and Long, G.L. (1989) *Anal. Biochem.* **180**, 147-151
17. Bornstein, P., and Balian, G. (1977) *Meth. Enzymol.* **47**, 132-45
18. Deng, W.P., and Nickoloff, J.A. (1992) *Anal. Biochem.* **200**, 81-8
19. Gill, S.C., and von Hippel, P.H. (1989) *Anal. Biochem.* **182**, 319-326
20. Mach, H., Middaugh, C.R., and Lewis, R.V. (1992) *Anal. Biochem.* **200**, 74-80
21. Ladokhin, A.S., Wang, S.L., Steggles, A.W., and Holloway, P.W. (1991) *Biochemistry* **30**, 10200-10296
22. Brzozowski, A.M., Pike, A.C.W., Dauter, Z., Hubbard, R.E., Bonn, T., Engström, O., Öhman, L., Greene, G.L., Gustafsson, J.A., and Carlquist, M. (1997) *Nature* **389**, 753-758.
23. Andrade, M.A., Chacón, P., Merelo, J.J., and Morán, F. (1993) *Prot. Eng.* **6**, 383-390
24. Scatchard, G. (1949) *Ann. N.Y. Acad. Sci.* **51**, 660-672

25. Hill, A.V. (1913) *Biochem. J.* **7**, 471
26. Peitsch, M. C. (1995) *Bio / Technology* **13**, 658-660
27. Peitsch, M. C. (1996) *Biochem. Soc. Trans.* **24**, 274-279
28. Guex, N. and Peitsch, M. C. (1997) *Electrophoresis* **18**, 2714-2723
29. Burstein, E.A., Vedenkina, N.S., and Ivkova, M.N. (1973) *Photochem. Photobiol.* **18**, 263-279
30. Eftink, M.R. and Ghiron, C.A. (1981) *Anal. Biochem.* **114**, 199-227

Appendix
Partial List of Plasmids Constructed

Plasmid	Insert Properties			Comments
	Start	End	Mutation	
pER08	301	551	None	Not designed to be hydroxylamine cleavable.
pER304	Gly+ 300	551	None	Somewhat heterogeneous cleavage by hydroxylamine K_d = 0.25±0.14 nM dissociation $t_{1/2}$ = 2.4 ± 0.4 hr
pER336	Gly+ 300	551	S305E	Homogeneous cleavage K_d = 0.17±0.06 nM dissociation $t_{1/2}$ = 1.2 ± 0.3 hr
pER348	Gly+ 300	551	N304D, S305E	Homogeneous cleavage K_d = 0.17±0.06 nM dissociation $t_{1/2}$ = 2.1 ± 0.5 hr
pER330	Gly-Arg+ 305	551	None	Homogeneous cleavage K_d = 0.20±0.04 nM dissociation $t_{1/2}$ = 2.2 ± 0.3 hr
pER335	Gly+ 306	551	None	Actual insert begins at estrogen receptor codon 300; contains S305G mutation to improve cleavage; Somewhat heterogeneous cleavage by hydroxylamine (additional cleavage site within MBP, in spite of mutation of MBP Asn-368) K_d = 0.19±0.08 dissociation $t_{1/2}$ = 1.4 ± 0.2 hr
pER337	Gly-Arg+ 315	551	None	Unstable; fusion protein binds estradiol, but rapidly loses activity during purification.
pER331	Gly+ 306	551	None	Actual insert begins at estrogen receptor codon 279; contains S305G mutation to improve cleavage; Somewhat heterogeneous cleavage by hydroxylamine (additional cleavage site within MBP)
pER333	Gly+ 306	551	None	Actual insert begins at estrogen receptor codon 300; contains S305G mutation to improve cleavage; Somewhat heterogeneous cleavage by hydroxylamine (additional cleavage site within MBP)
pER349	Gly-Arg+ 310	551	None	Somewhat unstable. K_d = 0.18±0.06 nM dissociation $t_{1/2}$ = 5.0 ± 2.2 hr; not changed by ligand binding.
pER03	301	567	None	Not designed to be hydroxylamine cleavable.

pER05	279	595		Not designed to be hydroxylamine cleavable. Poor expression; proteolytic degradation occurs within cells.
pER332	Gly-Arg+305	595	None	Poor expression; proteolytic degradation occurs within cells.
pER334	Gly-Arg+305	534	None	Heterogeneous cleavage Fusion protein K_d = 0.14
pER340	Gly+300	529	S305E	Unstable
pER350	Gly+300	534	S305E	Unstable
pER306	Gly+300	551	W360F	Unstable Fusion protein K_d = 1.56±0.21
pER316	Gly+300	551	W360Y	Fusion protein K_d = 0.52±0.01 Insufficiently stable for purification
pER307	Gly+300	551	W383F	K_d = 0.2 nM
pER308	Gly+300	551	W393F	K_d = 0.2 nM
pER310	Gly+300	551	W360F, W383F	Constructed and sequenced (expected to be unstable).
pER311	Gly+300	551	W360F, W383F	Constructed and sequenced (expected to be unstable).
pER312	Gly+300	551	W383F, W393F	K_d = 0.1 nM
pER313	Gly+300	551	W360F, W383F, W393F	Unstable
pER318	Gly+300	551	W360Y, W383F, W393F	Constructed and sequenced.
pER314	Gly+300	551	R503A	Unstable
pER315	Gly+300	551	L507R	Low level of protein expression (unstable?) Fusion protein K_d = 0.6
pER341	Gly+300	551	S305E, L509R	Constructed and sequenced.
pER317	Gly+300	551	S305E, C447W	Fusion protein K_d = ~1.6 (low but detectable activity in screening assay)
pER323	Gly+300	551	S305E, C381S	dissociation $t_{1/2}$ = 0.6 ± 0.1 hr This construct crystallizes

pER305	Gly+ 300	551	G366S	Fusion protein K_d = 0.45
pER11	279	567	A361V	Fusion protein K_d = 0.32
pER04	Gly+ 300	567	S433P	Estradiol binding detectable but very low (~100x below active constructs in screening assay).
pER370	Gly+ 300	551	Δ483-514	Extremely low activity in screening assay.
pER371	Gly+ 300	551	Δ474-505	Extremely low activity in screening assay.